CARDIFF UNIVERSITY
PRIFYSGOL CAERDYDD

ORCA – Online Research @ Cardiff

This is an Open Access document downloaded from ORCA, Cardiff University's institutional repository:https://orca.cardiff.ac.uk/id/eprint/105690/

This is the author's version of a work that was submitted to / accepted for publication.

Citation for final published version:

Motta, Davide, Sanchez Trujillo, Felipe Juan, Dimitratos, Nikolaos , Villa, Alberto and Prati, Laura 2018. An investigation on AuPt and AuPt-Bi on granular carbon as catalysts for the oxidation of glycerol under continuous flow conditions. Catalysis Today 308 , pp. 50-57. 10.1016/j.cattod.2017.10.012

Publishers page: http://dx.doi.org/10.1016/j.cattod.2017.10.012

Please note:
Changes made as a result of publishing processes such as copy-editing, formatting and page numbers may not be reflected in this version. For the definitive version of this publication, please refer to the published source. You are advised to consult the publisher's version if you wish to cite this paper.

This version is being made available in accordance with publisher policies. See http://orca.cf.ac.uk/policies.html for usage policies. Copyright and moral rights for publications made available in ORCA are retained by the copyright holders.

An investigation on AuPt and AuPt-Bi on granular carbon as catalysts for the oxidation of glycerol under continuous flow conditions

Davide Motta,[a] Felipe Sanchez,[a] Nikolaos Dimitratos,[a] Alberto Villa,[b] Laura Prati*,[b]

[a]Cardiff Catalysis Institute, School of Chemistry, Cardiff University, Main Building, Park Place, Cardiff, CF10 3AT, UK.

[b]Dipartimento di Chimica, Universitá degli studi di Milano, via Golgi 19, 20133, Milano, Italy

Corresponding author

Laura Prati

*email: Laura.Prati@unimi.it

Abstract

AuPt/AC and Bi modified AuPt/AC were prepared by impregnation using activated granular carbon as support followed by chemical reduction. The catalysts were characterized by means of Atomic Absorption Spectroscopy (AAS), transmission electron microscopy (TEM) and X-ray photoelectron spectroscopy (XPS). The catalysts were evaluated in the base free glycerol oxidation at mild reaction conditions in a continuous flow fixed bed reactor. Experimental parameters, such as, contact time (Liquid Hourly Space Velocity: LHSV), temperature and O_2 flow have been varied in order to evaluate catalytic performance in terms of activity, selectivity and long-term stability. Under optimized reaction conditions AuPt/AC showed a high selectivity to glyceric acid (68.3%) whereas Bi-AuPt/AC promoted the oxidation of the secondary alcohol giving a selectivity to dihydroxyacetone (DHA) of 48.1% at 28% conversion, one of the most promising values reported in the current literature. Long-term catalytic performance was carried out for 80 h and revealed a reasonable good stability of AuPt/AC against deactivation and leaching, whereas structural modification and subsequent changes in the catalytic reactivity were envisaged for Bi-AuPt/AC catalyst.

1. Introduction

The transformation of glycerol into valuable chemicals and fuels has attracted significant attention in recent years from both academia and industry research groups because of its high potential as a promising bio renewable sustainable chemical building block [1-4]. The annual production of glycerol has been estimated to be higher than 2 million tonnes per year [5] and the main process of production is via the synthesis of biodiesel by the transesterification process using oils and fats with methanol [6]. A range of significant chemical processes have been studied and proposed for the effective transformation of glycerol to a variety of valuable chemicals, such as dihydroxyacetone, glyceraldehyde, glyceric acid, glycolic acid, tartronic acid, hydroxypyruvic acid, lactic acid, acrylic acid using oxidation/dehydration processes (Scheme 1) [7-10]. Due to the diverse range of products one of the main challenges is to control activity, selectivity and stability during the chemical process. Several strategies have been employed to control product selectivity and activity based on the use of bimetallic and trimetallic nanoparticles [11]. Bimetallic Au-Pd, Au-Pt and trimetallic (Au-Pd-Pt) catalysts have shown to be more active than their monometallic counterparts, and achieving high selectivity for the selective production of glyceric and tartronic acids with improved stability in particular under mild base-free conditions [12-19]. One of the most desired and challenging intermediates of the glycerol oxidation process is the selective production of dihydroxyacetone, which is a primary product of the glycerol oxidation process [20]. Dihydroxyacetone is a valuable product extensively used in cosmetic, chemical and pharmaceutical industries and the industrial production of dihydroxyacetone is based on utilization of biocatalytic approaches with yields reaching 90% [21-23]. However, biocatalytic systems are working at specific reaction conditions and are sensitive to variation of experimental conditions, such as, pH, temperature and scale-up production. On the contrary, chemical heterogeneous catalysts and especially Pt- based ones offer the possibility to selectively oxidise glycerol at a range of broader experimental conditions but with lower yield to the desired products due to deactivation issues. Catalytic performance can be also affected from deactivation, poisoning and leaching of active

sites even the separation of products is easier than from an enzymatic broth. Previous reports have shown that Pt-based catalysts with the addition of Bi or Sb as promoters are promising approaches to produce dihydroxyacetone with significant levels of conversion and selectivity [24-29]. Recently we have reported the successful utilization of Bi-AuPd/C and Bi-AuPt/C catalysts synthesized by colloidal methods [30,31] for improving the selectivity in a range of alcohol and polyol oxidation reactions. In the case of glycerol oxidation and using a batch reactor configuration system and base-free conditions, we demonstrated the enhanced production of dihydroxyacetone as the main product with selectivity of 63% at 80% conversion. The synthesized Bi-AuPt/C catalysts showed improved catalytic stability than the Au-free Bi-Pt/C catalyst. Taking into account these promising results we extend our studies using continuous flow processes for exploring further the catalytic performance in terms of selectivity, activity and especially long-term stability of Au-Pt and Bi-AuPt catalysts. A range of experimental parameters have been varied such as contact time (Liquid Hourly Space Velocity: LHSV), temperature and O_2 flow to evaluate the catalytic performance and permit structure-activity investigations for getting insight into reaction pathways and possible role of Bi. Herein, we compared the activity of AuPt/AC and Bi-AuPt/AC catalysts. We demonstrate that the selectivity to glyceraldehyde or glyceric acid using AuPt/AC and to dihydroxyacetone using Bi-AuPt/C could be improved considerably by tuning particular experimental parameters of a continuous flow reactor. Finally, we report and discuss the long term catalytic performance of the AuPt/AC and Bi-AuPt/C, in terms of activity, selectivity, stability taking into account metal leaching and restructuring of active sites.

2. Experimental Section

2.1 Materials

$NaAuCl_4 \cdot 2H_2O$, K_2PtCl_4 and $BiO(NO)_3$ were from Aldrich (99.99% purity) and granular activated carbon (grain diameter 2-3 mm) ZM 85 W from Camel Chemicals. Before use the carbon was suspended in HNO_3 6 M to remove all metal impurities and ashes and left under stirring for 12 h, then washed several times with distilled water by decantation until the pH of the solution reached values of 6–6.5. Finally, the carbon was filtered off and dried for 5–6 h at 150 °C in static air. $NaBH_4$ of purity > 96% from Fluka, was used. Gaseous oxygen from SIAD was 99.99% pure.

2.2 Catalyst preparation

AuPt/AC

Solid $NaAuCl_4 \cdot 2H_2O$ (0.031 mmol) and K_2PtCl_4 (0.020 mmol) were dissolved in 100 mL of distilled H_2O. Granular activated carbon (1g) was added to the solution under stirring. The amount of support was calculated as having a metal nominal loading of 5 wt% with Au/Pt molar ratio of 8/2. The mixture was continuously stirred at room temperature for 2h till the solution turned from pale yellowed to colorless indicating full adsorption of the metal precursors on the support. The carbon was filtered and the solution was studied by AAS to determine the real metal loading. The solid was redispersed in 100 ml of distilled water and a 0.1 M fresh solution of $NaBH_4$ (metal/$NaBH_4$= 1:4 mol/mol) was added under stirring for a period of 30 minutes. The catalyst was filtered, thoroughly washed with distilled water (2 L) and dried at 100 °C in static air for 2h. The catalyst has been labeled as AuPt/AC.

Bi-AuPt/AC

Bismuth was added to a portion of AuPt/AC prepared with the methodology reported above. $BiO(NO)_3$ (0.012 mmol) was dissolved in 100 ml of distilled water at pH=2 (pH modified using concentrated H_2SO_4). Bi amount was calculated in order to have a final nominal loading of 0.5%. AuPt/AC was added to the solution and left under stirring for 2h. The slurry was filtered and the solution was studied by AAS to determine the real metal loading. The solid was redispersed in 100 ml

of distilled water and a 0.1 M fresh solution of $NaBH_4$ (metal/$NaBH_4$= 1:1 mol/mol) was added under stirring. The catalyst was filtered, thoroughly washed with distilled water (2L) and dried at 100 °C in static air for 2h. The catalyst has been labeled as Bi-AuPt/AC.

2.3 Catalytic test

Fixed bed reactor design: a reactor made by Pyrex with an inner diameter of 10 mm and a height of 100 mm, equipped with feed lines for supplying aqueous solution of glycerol (5 wt %) and molecular oxygen, an output line and a water jacket for heating was used. Dioxygen flow was regulated by mass flow and set at in 5, 10 and 15 mL/min. The reaction temperature was set at 30, 50 and 60 °C. The glycerol flow was set to have a Liquid Hourly Space Velocity (LHSV) of 0.023, 0.046, 0.092, 0.183, 0.368 h^{-1}. The catalyst (5g) was packed in the reactor and glycerol solution and oxygen fed at a constant flow rate concurrently from the top of the reactor at a controlled temperature. The reactor was fixed vertically to avoid channeling. The grain size was in the range of 2-3 mm.

Samples of 0.2 ml were taken periodically and analyzed by high-performance chromatography (HPLC) using a column (Alltech OA-10308, 300 mm x 7.8 mm) with UV and refractive index (RI) detection in order to analyze the mixture of the samples. H_3PO_4 0.1 wt % solution was used as eluent. The identification of the possible products was done by comparison with the original samples.

2.4 Catalyst characterisation

X-ray photoelectron spectra (XPS) was recorded on a Kratos Axis Ultra DLD spectrometer using a monochromatic Al Kα X-ray source. X-ray source (75-150W) and analyser pass energies of 160 eV (for survey scans) or 40 eV (for detailed scans). Samples for examination by transmission electron microscopy (TEM) were prepared by dispersing the catalyst powder in high purity ethanol using ultra-sonication. 40 µL of the suspension was dropped on to a holey carbon film supported by a 300 mesh copper TEM grid before the solvent was evaporated. The samples for TEM were then examined using a JEOL JEM 2100 TEM model operating at 200 kV. The actual metal content and metal leaching (Au, Pt, Bi) were checked by Atomic Absorption Spectroscopy (AAS) analysis of the filtrate, on a Perkin Elmer 3100 instrument.

3. Results and discussion

5 wt % AuPt/AC with Au/Pt 8/2 nominal molar ratio catalyst was prepared by impregnation method using $NaBH_4$ as reducing agent using granular activated carbon as support. Bi-AuPt/AC was prepared by adding 0.5 wt % Bi to AuPt/AC via impregnation of $BiO(NO)_3$ and followed by chemical reduction using $NaBH_4$. The exact metal loading was verified by AAS and the results presented in Table 1. Particle sizes and particle size distributions were determined from the TEM micrographs (Table 1, Figure 1b and 2b). AuPt/AC showed a mean size of 5.6 nm with a broad particle size distribution (Figure 1b). After the addition of Bi the mean size decreased to 3.9 nm and quite narrow particle distribution was observed (Figure 2b). This unexpected result could be explained as follow. Examining the particle size histograms (Figure 1 b and 2b), a higher fraction of nanoparticles smaller than 2 nm was observed after the addition of Bi. Such an unexpected evidence might be ascribed to the presence of small Au, Pt clusters in AuPt samples. These clusters are too small to be detected with the current TEM microscope used, but they coalesce after the addition of Bi at low pH (2) leading to the formation of few nanometer metal particles and to the apparent decrease in mean particle size. This trend was already observed after the washing of Au PVA nanoparticles deposited on carbon with acidic water [32]. XPS data and spectra performed on the catalysts are presented in Table 1 and Figure 3 respectively. The Atomic percentage at the surface of Au and Pt species is similar in both catalysts, 9.3% and 0.7%, respectively in the AuPt catalysts, and 9.6% and 0.7%, respectively in the Bi-AuPt one. It is evident that the AuPt atomic composition at the surface is different from the bulk, with the surface enriched in Au (Table 1). These results point out that Au and Pt are not present only as homogenous alloy nanoparticles and probably segregation of Au also occurred. It has not been possible to quantify any Bi content of both the fresh and used catalyst, this is probably because the low Bi content on the surface of the catalysts is below the detection limit of the instrument (Table 1). XPS spectra demonstrated that both Au and Pt are present in the metallic state (Figure 3) (BE of 84.2 and 71.5, for Au and Pt, respectively). Moreover, the Au 4f region has been scanned before and after the

total survey of the sample to compare for possible reduction of the AuClx species due to the exposure to X-ray beam. These scans do not exhibit any discernible variation on the spectra of Au 4f, therefore these results are in agreement with the absence of Cl on the surface validating the full reduction of Au^{3+} to Au^{0}.

The catalytic performance of the synthesized materials was evaluated in the liquid phase oxidation of glycerol in a continuous flow fixed bed reactor with the same reactor design previously used by our group to investigate the same reaction using monometallic Au catalysts [33]. A scheme of the reactor is illustrated in Scheme 2.

A range of experimental parameters have been varied such as contact time (LHSV), temperature and O_2 flow to evaluate the catalytic performance of the materials in terms of activity, selectivity and long-term stability (Table 2-7).

3.1 Catalytic performance of AuPt/AC

Table 2 shows the effect of the contact time (LHSV) on the activity and selectivity using AuPt/AC, keeping the O_2 flow and temperature constant (5 mL/min and 60°C, respectively). As expected by decreasing the contact time (increasing of LHSV), the conversion decreased from 34.5% (LHSV of 0.023 h^{-1}) to 8.6 (LHSV of 0.366 h^{-1}). At the lowest contact time (LHSV of 0.366 h^{-1}) the main products were glyceraldehyde (58.3%) and glyceric acid (34.1) (Table 2). By increasing the contact time, consecutive oxidation reactions were promoted (Scheme 2). At LHSV of 0.023 h^{-1} the majority of glyceraldehyde was oxidized to glyceric acid (51.4%) and sequentially to tartronic acid (23.1%). The highest selectivity to glyceric acid was obtained at LHSV of 0.046 h^{-1} (53.4%). With the aim to increase the productivity to glyceric acid, O_2 flow, was varied keeping constant LHSV (0.046 h^{-1}) and temperature (60 °C). Increasing O_2 flow from 5 to 15 mL/min the conversion did not significantly varied (from 24.2 to 29.2%) (Table 3). However, in presence of a higher amount of O_2 (15 ml/min) glyceraldehyde was mainly oxidized to glyceric acid, and a maximum of selectivity of 68% was reached. Finally, the effect of the temperature was evaluated (Table 4). Increasing the reaction temperature from 30 °C to 60 °C, an increase from 8.5 to 24.2 % conversion was obtained. A lower

temperature has a significant impact in the selectivity, limiting the consecutive oxidation of glyceraldehyde to glyceric acid. It is important to note that under all the reactions conditions tested AuPt/AC limits the formation of C1 and C2 products deriving from C-C cleavage. Indeed, the sum of C3 products (glyceraldehyde+glyceric acid + tartronic acid) was always >90%.

One of the main challenges for industrial applications of supported metal nanoparticles is the long-term catalytic performance and stability. Therefore, we investigated the stability of AuPt/AC catalyst against deactivation at reasonably long reaction times, following conversion and selectivity for 80 h of continuous flow reaction (Figure 4). We choose the reaction conditions were the highest selectivity to glyceric acid was obtained (LHSV=0.046 h^{-1}) T= 60 °C, O_2= 15 ml/min). The catalyst maintained similar levels of conversion and selectivity over a period of 80 h of reaction (Figure 4). At the end of the reaction the catalyst was removed from the reaction media and studied by means of AAS, TEM and XPS. The morphology of the used AuPt catalyst showed moderate structural modifications compared to the fresh one. AAS revealed a leaching of 2.6% of Au in the catalyst used after 80 h, whereas Pt content was the same (Table 1). TEM analysis showed that AuPt mean particle size did not change during the reaction (5.6 and 5.5 nm for AuPt nanoparticles before and after reaction, respectively) (Table 1). However, a small variation in the particle distribution were observed for the fresh and used catalysts(Figure 1b and 1d). Indeed, the particles smaller than 2nm observed in the fresh samples disappeared in the used one and a higher quantity of particles larger than 10 nm were present after reaction, although still was a minor fraction. XPS showed an increase of Au% at the surface after reaction (9.3 and 12.3% for fresh and used AuPt, respectively). A possible explanation is that part of Au present in Au pores is diffused from inside the pores of granular carbon and redeposited on the carbon surface and as consequence possible leaching was occurred and detected by AA analysis. XPS confirmed that also on the surface the content of Pt did not vary during the reaction. This result confirmed previous study showing that the addition of Au to Pt significantly enhance the stability of Pt in the liquid phase oxidation avoiding the leaching of the metal into the solution and the passivation [14].

3.2 Catalytic performance of Bi-AuPt/AC

As we stated previously the modification and addition of Bi is a well-known method to tune activity and especially block specific sites for tuning selectivity to desired products. The addition of Bi was carried out to study the possible role of Bi as a promoter and if this strategy as has been reported previously can facilitate the formation of primary products, such as, dihydroxyacetone. Comparing the activity and selectivity of AuPt/AC (Tables 2-4) and Bi-AuPtAC catalysts (Tables 5-7) it is evident that the addition of Bi significantly modified the reactivity of AuPt nanoparticles as already demonstrated in experiments performed previously in batch reactors [31]. The presence of a small amount of Bi (0.5wt %) increased the activity due most probably to the decrease of mean particle size and favored the oxidation of the secondary alcohol, with dihydroxyacetone (DHA) as main product (Tables 5-6). This observation could be attribute to the alteration of geometrical properties and blocking of active sites that Bi may introduce with a consequence the enhancement of desorption of dihydroxyacetone from the surface of the catalyst which results in the avoidance of consecutive oxidation to secondary products. In terms of activity the variation of contact time, conversion and temperature has a similar effect in both AuPt/AC and Bi-AuPt/AC. Indeed, also for Bi-AuPt/AC, an increase in the contact time and temperature resulted in a higher conversion, where the variation of O_2 flow did not significantly influenced the activity (Tables 5-7). In terms of selectivity, the highest one (48.1 %) to DHA at 24.5 % conversion was obtained at the lower contact times (LSHV 0.183 h^{-1}), with glyceric acid and glyceraldehyde (selectivity of 25.2% and 18.2 %, respectively) as main by-products (Table 5). Increasing the contact time the selectivity to DHA and glyceraldehyde decreased with the formation of formic and glycolic acid, deriving from C-C cleavage and hydroxypyruvic acid, produced by sequential oxidation of DHA (Scheme 1). Table 6 shows that higher O_2 flow had a detrimental effect on the selectivity to DHA. Indeed, increasing O_2 flow from 5 to 15 mL/min the selectivity to DHA decreased from 47.8% to 38.3 % due to the degradation of DHA to formic and glycolic acid and to its oxidation to hydroxypyruvic acid. At last, we observed an unexpected effect of the temperature. Indeed, the highest selectivity to DHA (47.8%) was obtained at 60°C, whereas at lower temperatures

(50°C and 30°C) DHA is prone to degrade to C1 and C2 products. This result is probably due to a lower desorption rate of DHA from the Bi-AuPt active sites at lower temperature, resulting in the sequential C-C cleavage.

The stability of Bi-AuPt was investigated under the reaction conditions giving the best selectivity to DHA (48.1%) (LHSV=0.183 h^{-1}) T= 60°C, O_2= 5 ml/min) (Figure 5) after 80 h of reaction. Both activity and selectivity to DHA decreased during the first 20 h, after which steady state conditions were obtained. The activity decreased from 24.5 to 18%, whereas the selectivity to DHA dropped from 48.1 to 40%) (figure 5). To better understand this observed catalytic behavior the used catalyst was thoroughly investigated. Both AAS and XPS confirmed that part of Bi was leached into the solution (Table 1). In particular, XPS showed that no Bi was present on the surface after 80 h of reaction. However, conversely to AuPt/AC catalyst, DHA remained the main product. We addressed this result to the fact that Bi is still partially present on the catalyst surface but under the detection limits of XPS apparatus used for this study could identified. TEM investigation on the used catalyst (Table 1, Figure 2c, 2d) showed a significant growth of metal particles from 3.9 to 8.1 nm. This result is unexpected due to the high stability of AuPt/AC catalyst presented above. We address this observation to a weaker metal -support interaction induced by the Bi presence with a consequent lower stability of AuPt nanoparticles than in the case of AuPt/AC.

4. Conclusions

AuPt/AC and Bi modified AuPt/AC catalysts were synthesized and tested in the base-free liquid phase oxidation of glycerol in a continuous flow fixed bed reactor. Reaction parameters (contact time, temperature and O_2 flow) were varied to evaluate the catalytic performance in terms of activity, selectivity and stability. Under optimized reaction conditions AuPt/AC showed a high selectivity to glyceric acid (68.3%) whereas Bi-AuPt/AC promoted the oxidation of the secondary alcohol resulting in a maximum of selectivity to DHA (48.1%). Stability tests performed for 80 h got new insight on the stability and structure of the two catalysts. Indeed, both catalytic results and characterization (AAS,

TEM, XPS) of AuPt/AC demonstrated the high stability of the catalyst. On the contrary, after modification of AuPt/AC with Bi, the catalyst showed significant structural modification after 80 h of time on stream. This result was addressed mainly due to a lower metal-support interaction induced by Bi addition. In subsequent studies we will focus on studying how the experimental conditions for the preparation if Bi-AuPt catalysts affect stability, metal composition of individual bimetallic nanoparticles and especially the location of Bi nanoparticles by means of HAADF and XAFS/XANES analysis. The presented studies address to a certain extent the issue of Bi stability, leaching and restructuring on preformed supported AuPt nanoparticles on an important biomass-derived molecule like glycerol and inspire future studies for the use of promoters like Bi and Sn.

References

1. P. Gallezot, Catal. Today, 37 (1997) 405-418.
2. G. W. Huber, A. Corma, Angew. Chem. Int. Ed. 46, (2007) 7184-7201.
3. A. Corma, S. Iborra, A. Velty, Chem. Rev. 107 (2007) 2411-2502.
4. M. Pagliaro, R. Ciriminna, H. Kimura, M. Rossi and C. Della Pina, Angew. Chem. Int. Ed. 46 (2007) 4434-4440.
5. R. Ciriminna, C. Della Pina, M. Rossi, M. Pagliaro, Eur. J. Lipid Sci. Technol. 116 (2014) 1432–1439.
6. C. H. C. Zhou, J. N. Beltramini, Y. X. Fan and G. Q. M. Lu, Chem. Soc. Rev. 37 (2008) 527-549.
7. A. Villa, N. Dimitratos, C. E. Chan-Thaw, C. Hammond, L. Prati, G. J. Hutchings, Acc. Chem. Res. 48 (2015) 1403−1412.
8. C.D. Evans, S.A. Kondrat, P.J. Smith, T.D. Manning, P.J. Miedziak, G.L. Brett, R.D. Armstrong, J.K. Bartley, S.H. Taylor, M.J. Rosseinsky, G.J. Hutchings, Faraday Discuss. 188 (2016) 427-450.

9. A. Chieregato, C. Bandinelli, P. Concepción, M.D. Soriano, F. Puzzo, F. Basile, F. Cavani, J.M. López Nieto, ChemSuChem 10 (2017) 234-244.
10. M. Morales, P.Y. Dapsens, I. Giovinazzo, J. Witte, C. Mondelli, S. Papadokonstantakis, K. Hungerbühlera, J. Pérez-Ramírez, Energy Environ. Sci. 8 (2015) 558-567.
11. M. Sankar, N. Dimitratos, P.J. Miedziak, P.P. Wells, C.J. Kiely, G.J. Hutchings, Chem. Soc. Rev. 41 (2012) 8099-8139.
12. W.C. Ketchie, M. Murayama, R.J. Davis, J. Catal. 250 (2007) 264-273.
13. W.C. Ketchie, Y.L. Fang, M.S. Wong, M. Murayama, R.J. Davis, J. Catal. 250 (2007) 94-101.
14. A. Villa, G. M. Veith, L. Prati, Angew. Chem. Int. Ed. 49 (2010) 4499-4502.
15. G. L. Brett, Q. He, C. Hammond, P. J. Miedziak, N. Dimitratos, M. Sankar, A. A. Herzing, M. Conte, J.A. Lopez-Sanchez, C.J. Kiely, D.W. Knight, S.H. Taylor, G.J. Hutchings, Angew. Chem. Int. Ed. 50 (2011) 10136-10139.
16. S.A. Kondrat, P.J. Miedziak, M. Douthwaite, G.L. Brett, T.E. Davies, D.J. Morgan, J.K. Edwards, D.W. Knight, C.J. Kiely, S.H. Taylor, G.J. Hutchings, ChemSusChem 7 (2014) 1326-1334.
17. A.Villa, S. Campisi, K.M.H. Mohammed, N. Dimitratos, F. Vindigni, M. Manzoli, W. Jones, M. Bowker, G.J. Hutchings, L. Prati, Catal. Sci. Tech. 5 (2015)1126-1132.
18. N. Dimitratos, A. Villa, L. Prati, C. Hammond, C.E. Chan-Thaw, J. Cookson, P.T. Bishop, Appl. Catal. A 514 (2016) 267-275.
19. S.M. Rogers, C.R.A. Catlow, C.E. Chan-Thaw, D. Gianolio, E.K. Gibson, A.L. Gould, N. Jian, A.J. Logsdail, R.E. Palmer, L. Prati, N. Dimitratos, A. Villa, P.P. Wells, ACS Catal. 5 (2015) 4377-4384.
20. F. Porta, L. Prati, J. Catal. 224 (2004) 397-403.
21. J. Tkac, Marian Navratil, E. Sturdık, P. Gemeiner, Enzyme and Microbial Technology 28 (2001) 383–388.
22. J.G. Hauge, T.E. King, V.H. Cheldelin, J. Biol. Chem. 214 (1995) 1–9.

23. O. Holst, S.O. Enfors, B. Mattiasson, Eur. J. Appl. Microbiol. Biotechnol. 14 (1982) 64–8.

24. H. Kimura, Appl. Catal. A 105 (1993) 147-158.

25. A. Abbadi, H. vanBekkum, Appl. Catal A. 148 (1996) 113-122.

26. H. Kimura, K. Tsuto, T. Wakisawa, Y. Kazumi and Y. Inaya, Appl. Catal. A 123 (1995) 323-323.

27. J. Gao, D. Liang, P. Chen, Z. Hou, X. Zheng, Catal Lett. 130 (2009) 185-191.

28. W. Hu, D. Knight, B. Lowry, A. Varma, Ind. Eng. Chem. Res. 49 (2010) (21) 10876-10882.

29. R. Nie, D. Liang, L. Shen, J. Gao, P. Chen, Z. Hou, Appl. Catal. B 127 (2012) 212-220.

30. A. Villa, D. Wang, G.M. Veith, L. Prati, 292 (2012) J. Catal. 73-80.

31. A. Villa, S. Campisi, C. E. Chan-Thaw, D. Motta, D. Wang, L. Prati, Catal. Today 249 (2015) 103–108.

32. S. Campisi, C. E. Chan-Thaw, D. Wang, A. Villa, L. Prati, Catal. Today, 278 (2016) 91–96.

33. A. Villa, C.E. Chan-Thaw, L. Prati, Appl. Catal. B: Environmental 96 (2010) 541–547.

Table 1. Characteristics of AuPt based catalysts

Catalyst	Metal loading (wt %)		TEM		XPS % at		
	Nominal Au-Pt-Bi	Determined by AAS Au-Pt-Bi	Mean size (nm)	Standard deviation σ	Au	Pt	Bi
AuPt/AC fresh	4.0-1.0-0.0	3.8-0.8-0.0	5.6	2.2	9.3	0.7	-
AuPt/AC used	4.0-1.0-0.0	3.7-0.8-0.0	5.5	1.9	12.3	0.7	-
Bi-AuPt/AC fresh	4.0-1.0-0.5	3.7-0.8-0.4	3.9	1.5	9.6	0.7	-
Bi-AuPt/AC used	4.0-1.0-0.5	3.6-0.7-0.2	8.1	3.6	10.9	0.9	-

Table 2. Effect of glycerol flow for AuPt/AC

LHSV (h^{-1})	Conversion (%)	Selectivity					
		Dihydroxy-acetone	Glyceric acid	Glyceral dehyde	Glycolic acid	Tartronic acid	Formic acid
0.023	34.5	0.7	51.4	14.3	5.2	23.1	0.8
0.046	24.2	0.6	53.4	23.6	3.9	16.8	0.9
0.092	15.9	1.2	47.1	35.8	1.3	9.4	0.8
0.183	14.1	1.2	38.2	53.3	1.2	4.1	1.0
0.366	8.6	1.4	34.1	58.3	0.9	1.3	0.9

Reaction conditions: glycerol 5 wt%, O_2 flow 5mL/min, T=60°C

Table 3. Effect of O_2 flow for AuPt/AC

O2 flow	Conversion (%)	Selectivity					
		Dihydroxy-acetone	Glyceric acid	Glyceral dehyde	Glycolic acid	Tartronic acid	Formic acid
5	24.2	0.6	53.4	23.6	3.9	16.8	0.9
10	27.3	0.3	64.2	10.3	4.1	18.2	1.2
15	29.2	0.1	68.3	5.2	5.9	19.4	0.8

Reaction conditions: glycerol 5 wt%, T=60°C, LHSV= 0.046

Table 4. Effect of temperature for AuPt/AC

Reaction temperature °C	Conversion (%)	Selectivity					
		Dihydroxy-acetone	Glyceric acid	Glyceral dehyde	Glycolic acid	Tartronic acid	Formic acid
30	8.5	1.2	55.3	33.1	1.5	6.7	0.8
50	20.3	0.5	50.2	29.3	2.5	14.3	0.5
60	24.2	0.6	53.4	23.6	3.9	16.8	0.9

Reaction conditions: glycerol 5 wt%, O_2 flow 5mL/min, LHSV 0.046

Table 5. Effect of glycerol flow for Bi-AuPt/AC

LHSV (h^{-1})	Conversion (%)	Selectivity					
		Dihydroxy-acetone	Glyceric acid	Glyceral dehyde	Glycolic acid	Formic acid	Hydroxy pyruvic acid
0.023	36.9	40.2	27.6	7.3	10.3	5.4	7.8
0.046	31.2	43.2	29.4	8.9	5.8	3.9	6.7
0.092	28.5	47.8	26.3	14.1	3.2	2.3	4.2
0.183	24.5	48.1	25.2	18.2	2.2	1.8	3.1
0.368	21.3	46.9	22.4	24.3	1.8	0.6	2.4

Reaction conditions: glycerol 5 wt%, O_2 flow 5mL/min, T=60°C

Table 6. Effect of O_2 flow for Bi-AuPt/AC

O2 flow	Conversion (%)	Selectivity					
		Dihydroxy-acetone	Glyceric acid	Glyceral dehyde	Glycolic acid	Formic acid	Hydroxy pyruvic acid
5	28.5	47.8	26.3	14.1	3.2	2.3	4.2
10	29.4	42.5	25.4	7.8	8.9	8.2	5.8
15	31.5	38.3	23.1	3.4	14.3	12.2	7.1

Reaction conditions: glycerol 5 wt%, O_2 flow 5mL/min, T=60°C

Table 7. Effect of temperature for Bi-AuPt/AC

Reaction temperature °C	Conversion (%)	Selectivity					
		Dihydroxy-acetone	Glyceric acid	Glyceral dehyde	Glycolic acid	Formic acid	Hydroxy pyruvic acid
30	9.3	31.2	20.3	17.8	12.2	7.9	8.1
50	20.7	37.5	24.4	16.8	5.4	6.8	7.9
60	28.5	47.8	26.3	14.1	3.2	2.3	4.2

Reaction conditions: glycerol 5 wt%, O_2 flow 5mL/min, LHSV

Figure 1 a) Representative TEM images and b) particle distribution of fresh AuPt/AC. c) Representative TEM images and d) particle distribution of AuPt/AC after reaction

a)

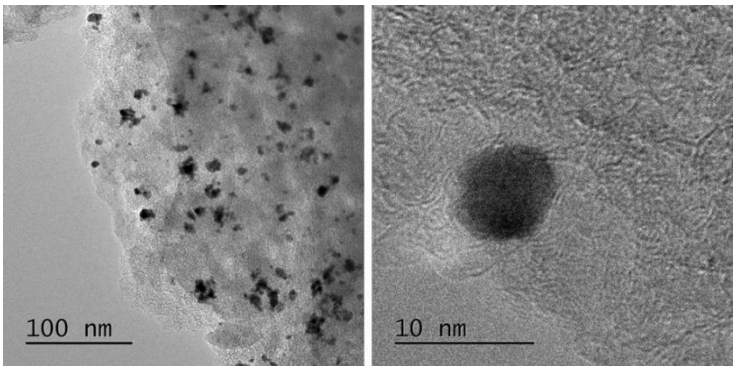

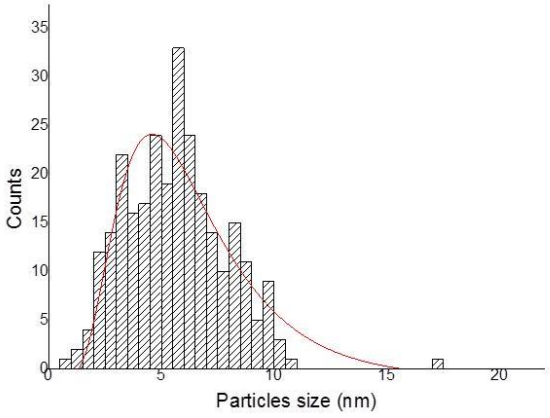

b)

c)

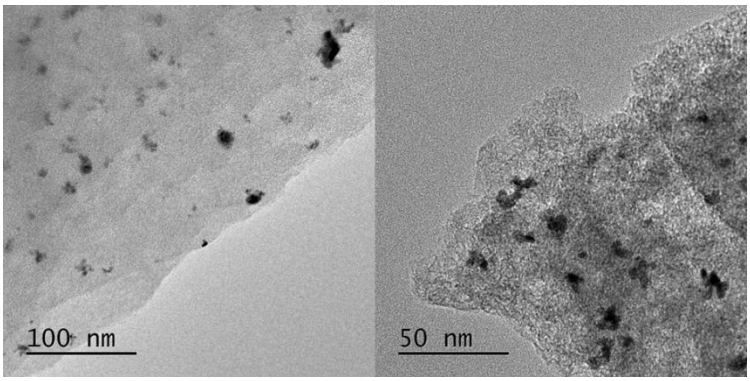

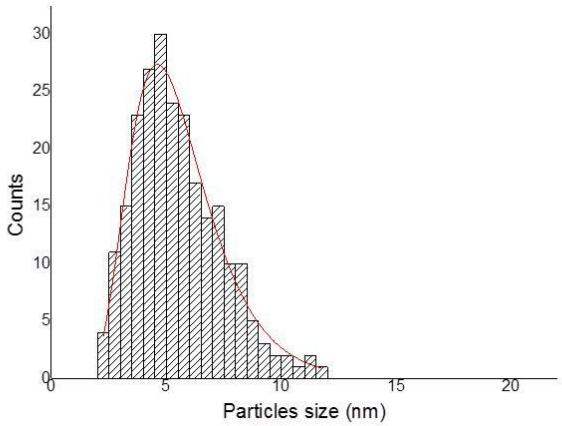

d)

Figure 2 a) Representative TEM images and b) particle distribution of fresh Bi-AuPt/AC.
c) Representative TEM images and d) particle distribution of Bi-AuPt/AC after reaction

a)

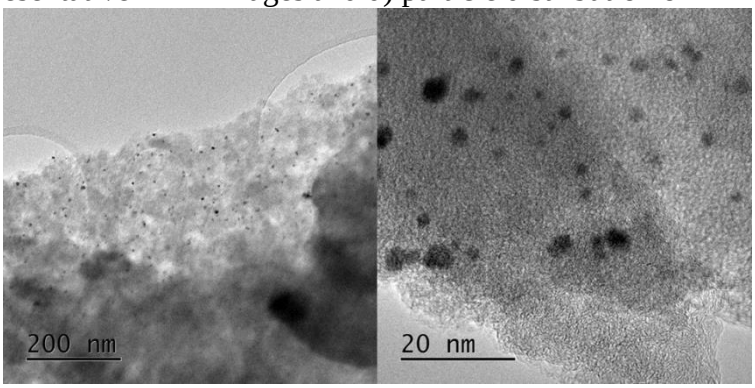

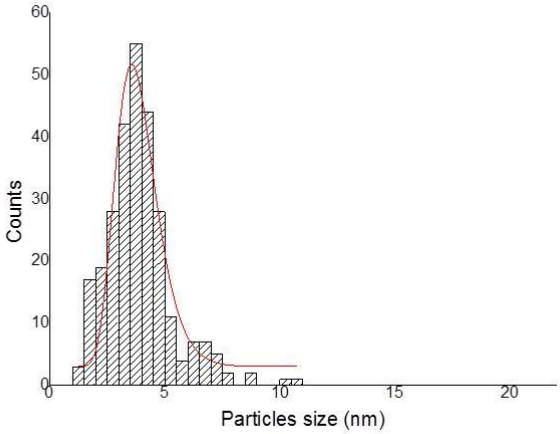

b)

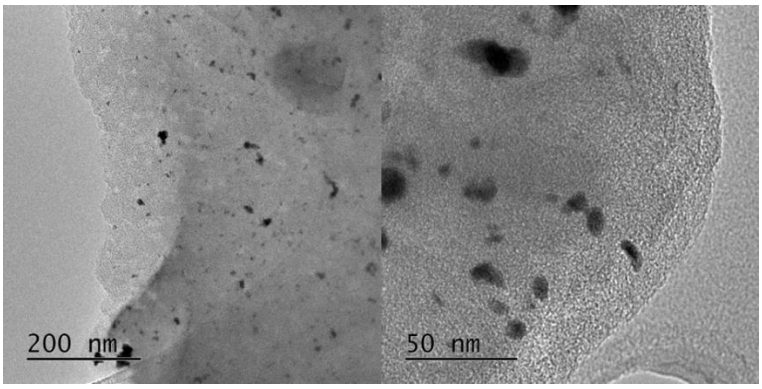

c)

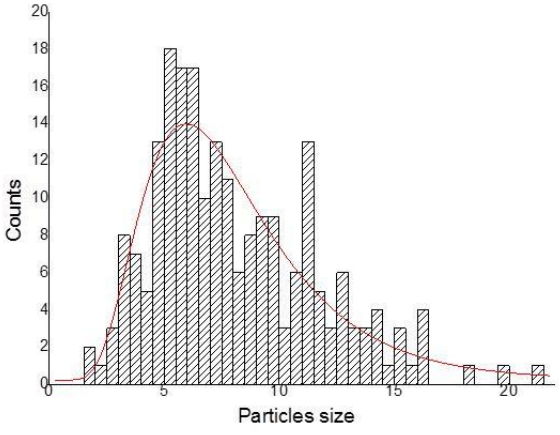

d)

Figure 3 XPS spectra of a) AuPt/AC and b) Bi-AuPt/AC

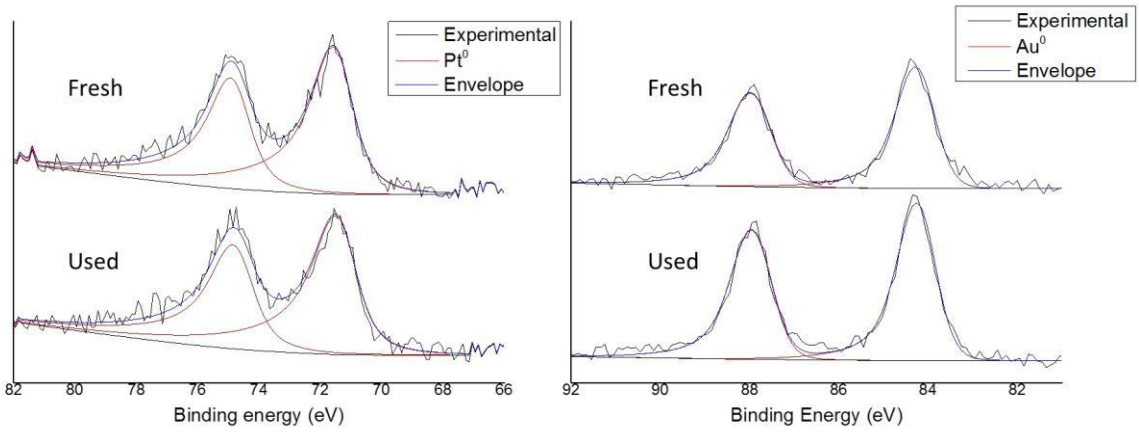

a)

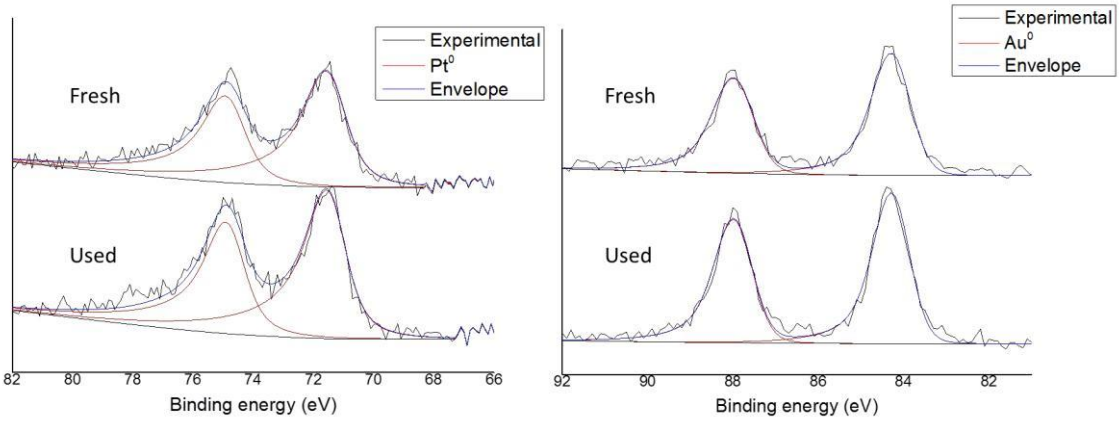

b)

Figure 4 Long term stability test in the glycerol oxidation using AuPt/AC

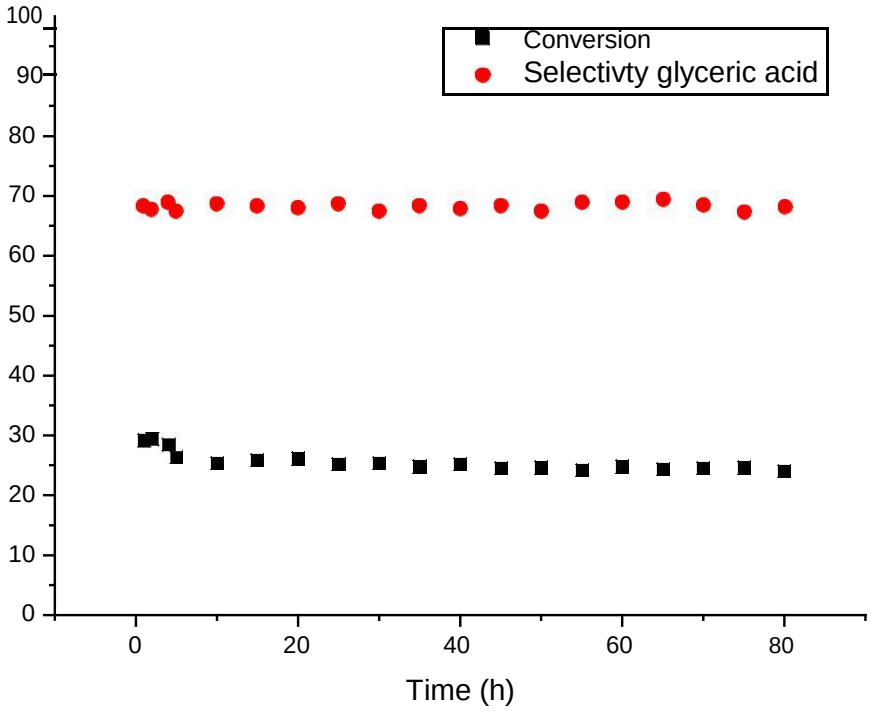

Figure 5 Long term stability test in the glycerol oxidation using Bi-AuPt/AC

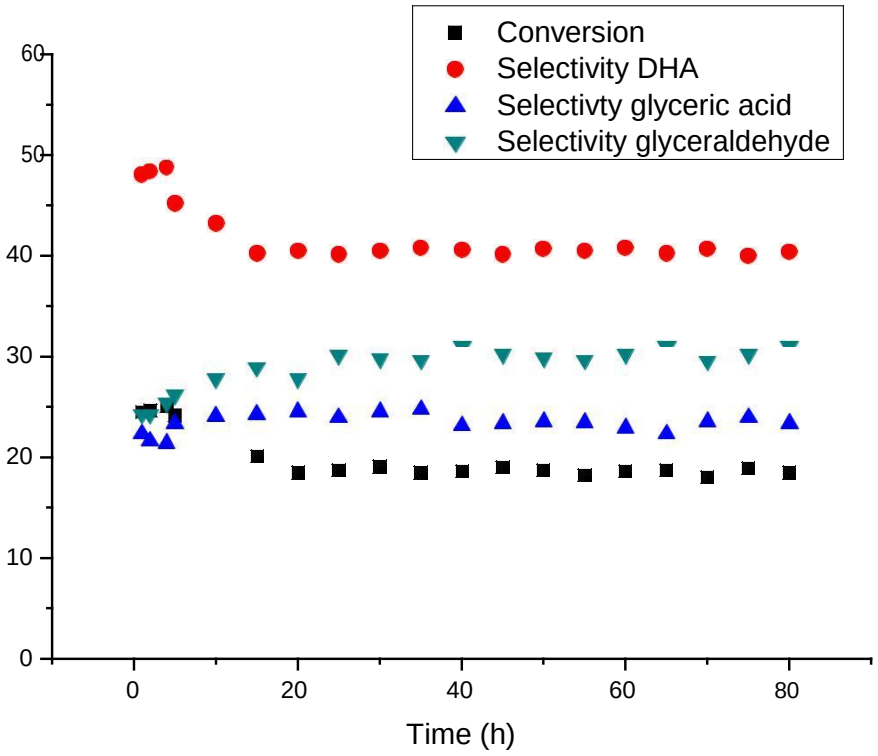

Scheme 1

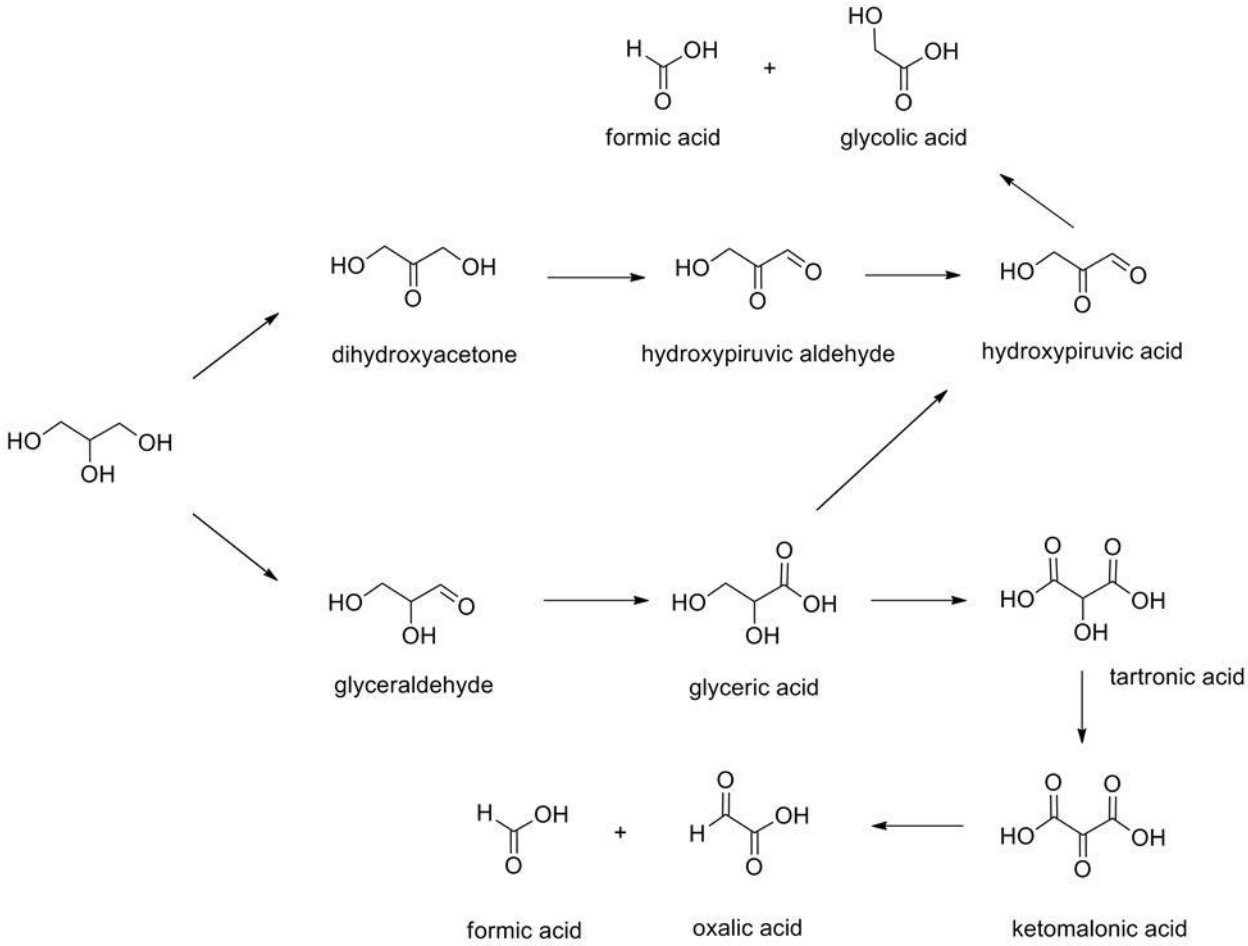
formic acid
glycolic acid
dihydroxyacetone
hydroxypiruvic aldehyde
hydroxypiruvic acid
glyceraldehyde
glyceric acid
tartronic acid
formic acid
oxalic acid
ketomalonic acid

Scheme 2

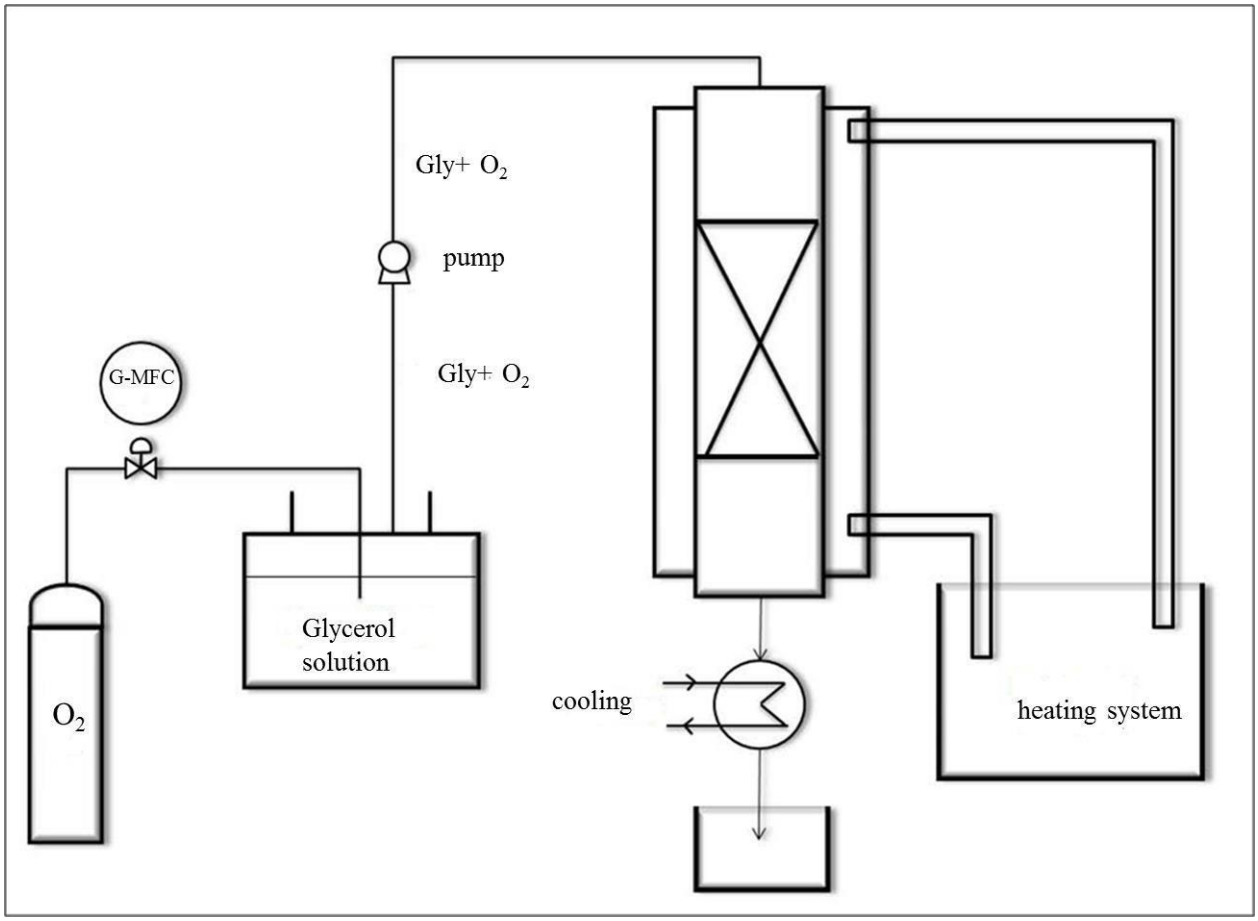
Gly+ O_2
pump
Gly+ O_2
G-MFC
Glycerol solution
O_2
cooling
heating system